Dottorato di Ricerca in Fisica XXXI ciclo

Dottoranda: Marilena Giglio

Titolo progetto di ricerca: **TECNICHE SPETTROSCOPICHE INNOVATIVE PER LA RIVELAZIONE DI TRACCE GASSOSE**

Tutor: Prof. Vincenzo Spagnolo

Second year PhD report

Quartz-enhanced photoacoustic spectroscopy (QEPAS) is a spectroscopic technique that combines the benefits of the photoacoustic spectroscopy with those of a high-Q quartz tuning fork (QTF), providing an ultra-compact, robust, and cost-effective trace gas sensing module. This method is based on photo-acoustic effect, i.e., heat conversion of light absorbed by a gas target via molecular collision-induced non-radiative relaxation of excited states. This heating causes the gas to expand and, if the light is modulated, the periodic expansion produces pressure waves, i.e. sound, that can be detected. QEPAS is based on the use of a quartz tuning fork (QTF) resonator as an optoacoustic transducer and the frequency of the light modulation has to match the QTF resonance frequency or one of its sub-harmonics. Until 2013, all QEPAS sensors reported in literature made use of standard commercial QTFs designed to vibrate at a resonance frequency of 32,768 (2^{15}) Hz. Recently, custom QTFs properly designed to optimize the sensing performances have been employed in sensing systems.

During the second year of the PhD, the research activity has been focused on the design, realization and characterization of QEPAS gas sensors employing custom QTFs, in order to target:

- ethylene at sub-ppm concentrations;
- a set of absorption lines of methane;
- two broad absorbtion bands of nitrous oxide.

In standard QEPAS, the QTF is coupled with two microresonator tubes with the aim of enhancing the signal to noise ratio. We recently developed a new spectrophone configuration, in which a single tube, set between the QTF prong is employed, leading to a further enhancement of the the QTF signal.

Finally, we theoretically predicted the best coupling conditions of tapered Hollow-core waveguides with laser sources in the mid-infrared spectral range and experimentally demonstrated the low-loss single mode laser beam delivery of tapered fibers within the range 3.5 - 7.8 μm.

Compact quartz-enhanced photoacoustic sensor for sub-ppm ethylene detection in atmosphere

Among the hydrocarbons, Ethylene (C_2H_4) is one of the most basic chemical building blocks: processing chemical plants turn it into polyethylene, polyester, PVC, polystyrene, ethylene glycol. Ethylene detection is thus fundamental for even rising demand of this gas.

We exploited the QEPAS technique for the detection and the quantification of ethylene, realizing a compact Thorlabs parts-based QEPAS system (see Figure 1), to allow in situ monitoring.

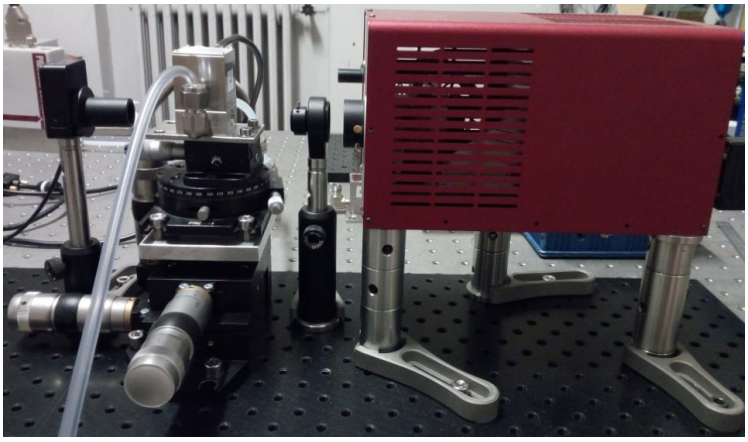

Figure 1: Picture of the compact ethylene QEPAS sensor.

We employed a custom QTF operated at the first overtone mode, having resonance frequency of 21503 Hz and quality factor of 23900 at 120 Torr, coupled with 2 microresonator tubes (Length: 4 mm, Inner diameter: 0.84 mm Outer diameter: 1.65 mm). The targeted ethylene absorption line falls at 966.38 cm^{-1} with a line strength of 2.2 10^{-20} cm/mol. The optical power focused between the QTF prongs was 74 mW. With a certified concentration of 100 ppm in N_2, we measured a signal of 85.84 mV and a noise of 0.086 mV, with an integration time of 100ms, leading to a minimum detection limit of 100 ppb. By means of the Allan deviation analysis, we estimated a noise reduction down to 0.026mV when using an integration time of 10 s, with an ultimate detection limit of 30 ppb. The Allan deviation plot is shown in Figure 2.

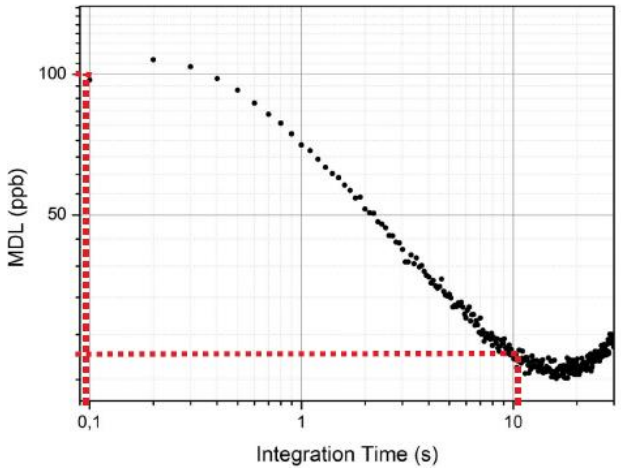

Figure 2: Allan deviation plot reporting the minimum detection limit achievable by using 100 ms and 10 s integration time.

We also calibrated the sensor by acquiring the QEPAS signal corresponding to different ethylene concentrations, obtained by diluting the certified 100 ppm concentration. The obtained spectral scans are reported in Figure 3 (a). From the calibration curve reported in Figure 3 (b), a QEPAS signal variation of 0.85 mV per ppm was calculated.

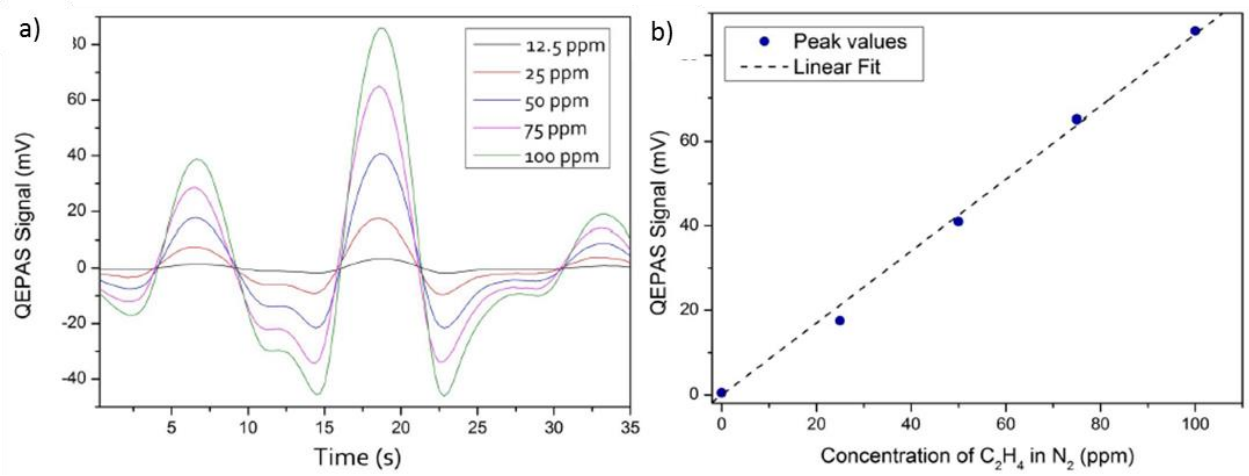

Figure 3: Spectral scans of ethylene at different concentrations (a) and calibration curve obtained by fitting the peak values measured from the spectral scans (b).

Quartz-enhanced photoacoustic gas sensor employing a broad-band laser source in pulsed operation

Currently, most spectroscopic instruments based on quantum cascade lasers (QCLs) use single-mode Distributed-Feedback (DFB) lasers with limited tuning range (at most 15 cm^{-1}) or external cavity semiconductor devices that are limited in full broadband tuning speed to up to only a few

scans per second. In addition, external cavity devices are limited in fieldability due to the necessity of moving gratings and output couplers, compromising tuning robustness and repeatability.

We realized a gas sensor based on quartz enhanced photoacoustic spectroscopy (QEPAS) employing a broadband source composed by a monolithic array of 32 DFB QCLs, packaged in a single module with temperature control, electronic drivers and beam combining optics. The broadband source emits in pulsed mode from 1200 to 1310 cm^{-1}. The frequency spacing between consecutive QCL emitters is ~ 4 cm^{-1} and each one can be tuned of ~ 3 cm^{-1} by linearly varying the temperature from 15° C to 50 °C. The linewidth of each QCL emission is ~ 1.5 cm^{-1}. The QCLs emission spectra are shown in Figure 4 (a). The acoustic detection module is composed by a custom QTF operating at 25.4 kHz and having 1 mm prong spacing, properly selected to be adapted to the poor spatial quality of the focused laser beam profiles and to be not affected by the beam steering effect when the source is switched from one QCL to another one. We targeted the two broad spectral bands of nitrous oxide and several absorption lines of methane falling in the 1200 - 1310 cm^{-1} spectral range, whose absorption coefficients are shown in Figure 4 (b).

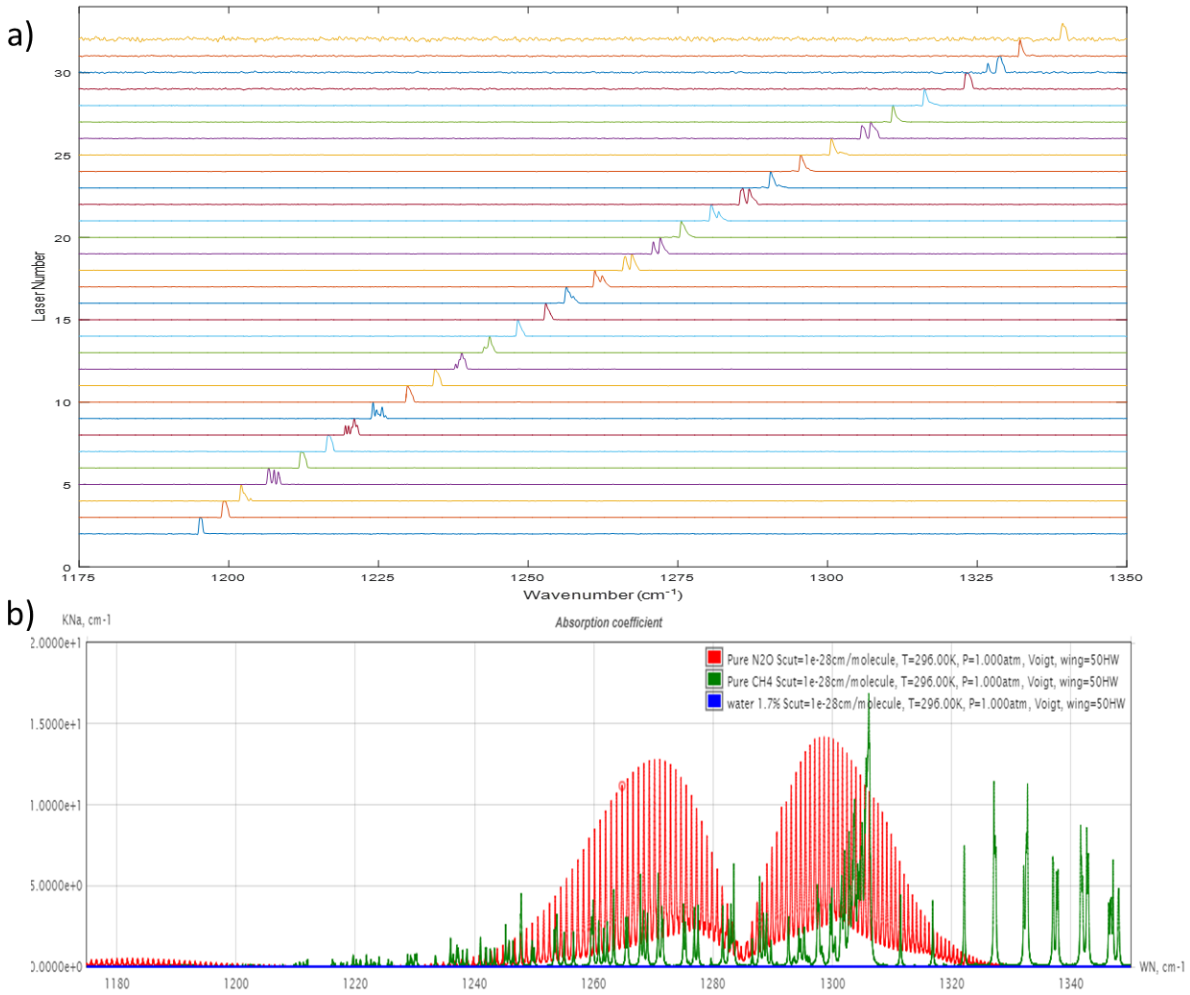

Figure 4: QCLs emission spectra a) and simulated 1.7% water vapour (blue), pure N_2O (red) and pure CH_4 (green) Absorption coefficient.

By rapidly switching the QCL sources, the QEPAS sensor was used to detect pure N_2O, pure CH_4 and a mixture of 50% N_2O and 50% CH_4 at atmospheric pressure. The measured QEPAS signal, normalized to the optical power of the QCLs, are shown in Figure 5.

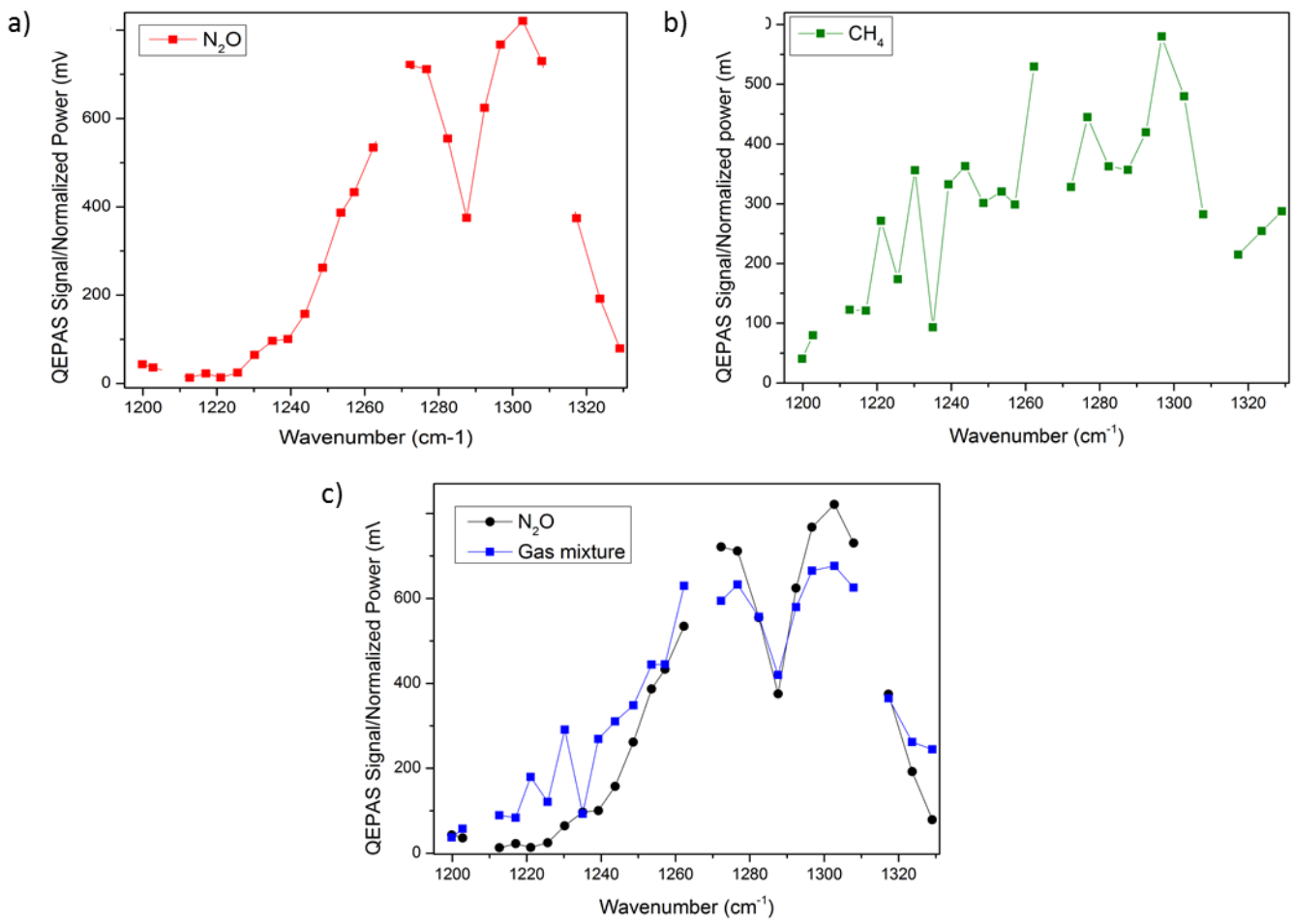

Figure 5: QEPAS Signal/Normalized power when switching the QCLs, when targeting pure N_2O (a), pure CH_4 (b) and a 50% N_2O-50% CH_4 mixture, at atmospheric pressure.

It can be observed that the acquired QEPAS signal well reproduces the two broad spectral bands of the N_2O. It is also possible to recognise some absorption structures of the CH_4. Finally, the trend of the acquired data for the gas mixture follows the trend of the absorption coefficient: some CH_4 peaks appear over the N_2O band.

Single-tube on beam quartz-enhanced photoacoustic spectrophones exploiting a custom quartz tuning fork operating in the overtone mode

Custom tuning forks opened the way to two novel approaches to increase the sensing performance of a QEPAS spectrophone. First, QTFs with larger prongs made it possible to accommodate between them a single-tube resonator (SO-QEPAS), with a pair of slits realized

where the acoustic pressure antinode is located. With this approach, the size of the QEPAS spectrophone was reduced with respect to a dual-tube configuration. Secondly, QTFs can be specifically designed to enhance the first overtone mode providing a higher quality factor with respect to the fundamental mode. We combined these two approaches and investigated the sensing performance of a single-tube on-beam QEPAS spectrophone exploiting a custom QTF operating in the overtone mode.

Based on previous studies on the influence of the QTF geometry on the resonance frequency and quality factor, we designed a custom QTF having prongs 19 mm long, 1.4 mm wide and 0.8 mm thick with a prong spacing of 1 mm. We measured a fundamental mode resonance frequency of 4250 Hz with a quality factor of 10700 and a first overtone mode resonance frequency of 25413 Hz with a quality factor of 28950, ~2.7 times higher than that measured for the fundamental mode. The single-tube on-beam configuration is obtained by setting a resonator tube between the QTF prongs, as shown in Figure 6(c). The tube surface thickness is polished in order to reduce the outer diameter and to allow the tube to be positioned between the prongs, as shown in Figure 6 (b). A pair of slits is opened on each side of the tube waist, as highlighted in Figure 6 (a), symmetrically in the middle of the tube, where the acoustic pressure antinode is located. The sound wave exiting from two slits impacts on the internal surface of two prongs and excites in-plane anti-symmetrical vibrational modes.

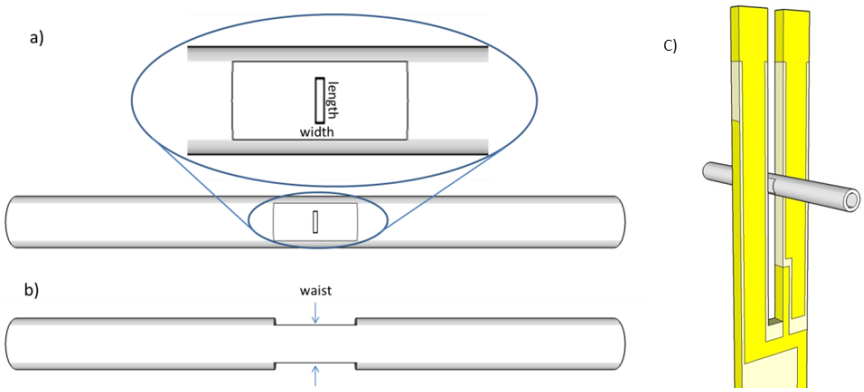

Figure 6: Front (a) and top (b) view of the single micro-resonator tube and resonator single-tube on beam configuration (c).

We analysed in detail how the geometry of the resonator tube influences the sensing performance of the QEPAS spectrophone. With this aim, four micro-resonators characterized by different internal diameters (0.67 mm, 0.80 mm, 0.88 mm and 0.96 mm) with the same length l (10.8 mm) and slit width (100 µm) were tested. The highest QEPAS signal (33.5 mV) was obtained with tube having inner diameter ID = 0.88 mm. For an ID = 0.88 mm, the QEPAS performance at different tube lengths (slit sizes were not changed), ranging from 13.3 mm (~λ) to 7 mm (~λ/2) was investigated. The maximum QEPAS signal of 33.9 mV was obtained for an optimal tube length of 11.0 mm. The observation of an optimal tube length > λ/2 is a clear evidence that the 1st harmonic acoustic standing waves in the tube were partially distorted by

the two slits present in the acoustic resonator, as observed in previous SO-QEPAS experiments. Finally, for the ID = 0.88 mm and an l = 10.8 mm we enlarged the slit width without changing its length. The QEPAS signal increased up to 61.7 mV when the slit width was 250 µm, almost twice with respect to a slit width of 100 µm. With these conditions, we measured a SO-QEPAS signal 40 times higher with respect to a bare QTF, as shown in Figure 7.

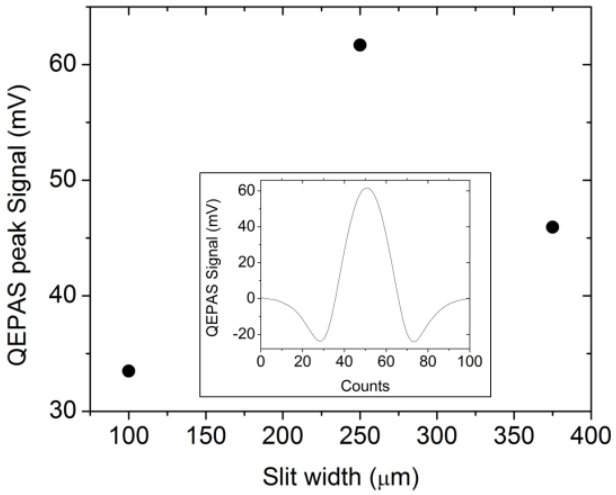

Figure 7. QEPAS peak signal recorded for three different slit widths. In all three cases, the tubes were 10.8 mm long, with the ID of 0.88 mm and the slit length of 0.9 mm. Inset: SO-QEPAS spectral scan of the selected water line with the QTF operating with the overtone mode with the tube ID of 0.88 mm, length of 11.0 mm and a slit width of 250µm.

Low-loss and single-mode tapered hollow-core waveguides optically coupled with interband and quantum cascade lasers

Hollow-core waveguides (HCWs) are optical fibers which guide light essentially within a cylindrical hollow region surrounded by a tube via multiple reflections at layers deposited within the tube. Driven by the lack of low-absorption materials for solid-core fibers, HCWs recently found applications as laser beam delivery to guide light in mid-infrared spectral range. We investigated the properties a HCW with a tapered bore profile, i.e., with the bore radius linearly increasing from a_1 = 100 µm to a_2 = 130 µm, in a 50 cm fiber length L, as shown in Figure 8. The tapered fiber was coupled by using an interband cascade laser emitting at 3.5 µm and four quantum cascade lasers emitting at 4.6 µm, 5.2 µm, 6.2 µm and 7.8 µm, respectively,in order to investigate the optical performances of the HCWs within a wide spectral range.

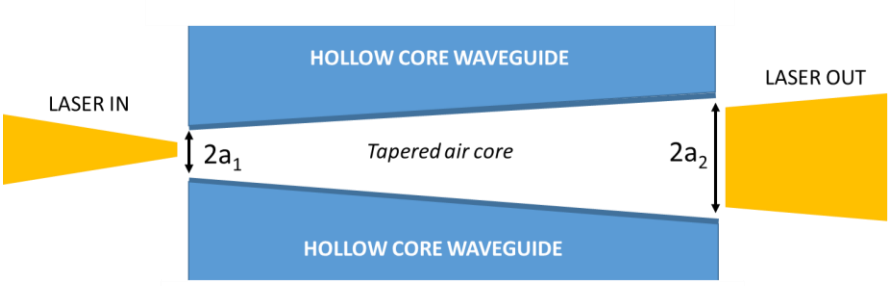

Figure 8 Sketch of the Longitudinal section of the tapered HCW. The air core diameter increases linearly from 2a1 = 200 µm to 2a1 = 260 µm, for a total fiber length of 50 cm.

The propagation losses and the quality of the out-coming beam are strongly influenced by the optical coupling conditions between the laser beam and the HCW. When a lens is used to couple a collimated laser beam into the waveguide entrance, the selection of its focal length is mainly determined by the beam diameter, the laser wavelength and the HCW bore diameter. By supposing a fixed collimated beam diameter, a single focal length could not allow optimal coupling conditions to be maintained within a wide spectral range of operation. We performed theoretical calculations to identify the best HCW-laser coupling conditions in terms of optical losses and single-mode fiber output, by using both fiber sides as HCW input (i.e., coupling into the smaller end versus coupling into the larger end).

When a Gaussian beam G(r) is focused into a hollow waveguide along the optic axis, only the hybrid HE1m modes, which can be approximated by the zero order Bessel functions $J(u_{1m}\, r/a)$, are excited inside the waveguide. The best coupling condition is obtained by maximizing the input laser mode coupling into the HE_{11} waveguide hybrid mode, providing the lowest theoretical losses and characterized by a Gaussian-like optical power distribution. The amount of the optical power coupled with the first waveguide mode can be expressed in terms of the power coupling efficiency η_{11}. We calculated the η_{11} coupling efficiency as a function of the laser wavelength, considering a_1 or a_2 as input bore radius.

$$\eta_{11} = \frac{\left| \int_0^a G(r) J\left(u_{11} \frac{r}{a} \right) r dr \right|^2}{\int_0^a G^2(r) r dr \int_0^a J^2\left(u_{11} \frac{r}{a} \right) r dr}$$

The results are shown in Figure 9.

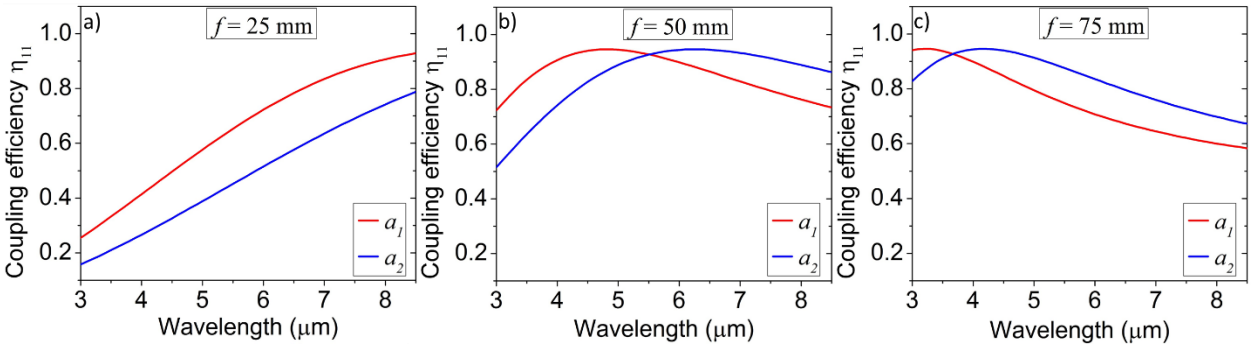

Figure 9: η_{11} coupling efficiency calculated as a function of the laser wavelength, when the input beam is coupled through the a1 (red line) or a2 (blue line) input side, using a coupling lens with f = 25 mm, f = 50 mm or f = 75 mm, respectively.

To estimate the propagation losses, we employed the equation derived by Miyagi and Kawakami to determine the attenuation coefficients α_{1m} for the HE_{1m} waveguide modes, considering that the inner core radius a(z) varies linearly along the waveguide length L.

$$L_p(dB) = -10Log_{10}\left(\sum_m \eta_{1m}\exp\left(-2\int_0^L \alpha_{1m}(z)dz\right)\right)$$

We calculated Lp values as a function of the wavelength with f = 25 mm, f = 50 mm and f = 75 mm, respectively, as reported in Figure 10.

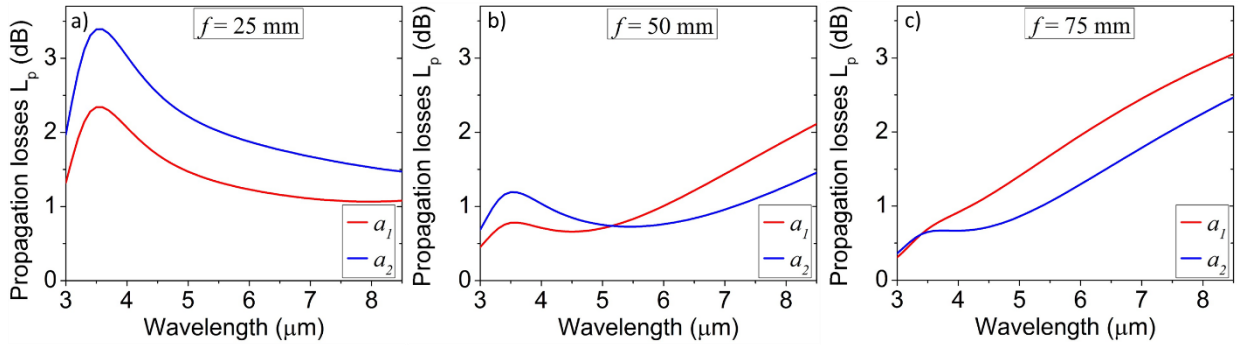

Figure 10: Propagation losses Lp as a function of the wavelength when the laser beam is focused into a1 (red line) or a2 (blue line), using a lens with f = 25 mm, f = 50 mm or f = 75 mm, respectively.

For each laser source and each focal length, we used the theoretical model to evaluate the coupling efficiency and the propagation losses when the laser beams are coupled to the a_1 or a_2 HCW sides. Single-mode Gaussian-like beam profiles at the HCW exit were obtained for all the employed light sources, even if using the bigger a_2 as input side. This confirms that tapered HCWs allow using larger bore size for single-mode operation with respect to standard HCW, thereby facilitating the fiber-laser alignment.

List of publications

1) Giglio, M., Patimisco, P., Sampaolo, A., Kriesel, J.M., Tittel, F.K. and Spagnolo, V. Low-loss and single-mode tapered hollow-core waveguides optically coupled with interband and quantum cascade lasers. Optical Engineering, 57(1), p.011004 (2017).

Conference Proceedings

1) Giglio, M., Sampaolo, A., Patimisco, P., Zheng, H., Wu, H., Dong, L., Tittel, F.K. and Spagnolo, V., Single-tube on beam quartz-enhanced photoacoustic spectrophones exploiting a custom quartz tuning fork operating in the overtone mode, SPIE OPTO, 2017
2) Sampaolo, A., Patimisco, P., Gluszek, G., Hudzikowski, A., Giglio, M., Zheng, H., Tittel, F.K. and Spagnolo, V., Low power consumption quartz-enhanced photoacoustic gas sensor employing a quantum cascade laser in pulsed operation, SPIE OPTO, 2017

Conference Talks

1) Tittel, F.K., Spagnolo, V., Patimisco, P., Giglio, M., Sampaolo, A., Ye, W., He, Q., Zheng, H., and Lou, M., Recent Advances and Applications of Mid-infrared Cavity and Quartz Enhanced Photoacoustic Spectroscopy, Mirsens, 2017
2) Sampaolo, A., Patimisco, P., Zheng, H., Giglio, M., Dong, L., Tittel, F.K. and Spagnolo, V., Recent Advances In Quartz-Enhanced Photoacoustic Sensors Employing Custom Tuning Fork Operating At The First Overtone Flexural Mode, CLEO Europe, 2017
3) Spagnolo, V., Sampaolo, A., Patimisco, P., Zheng, H., Giglio, M., Dong, L., Tittel, F.K., New developments in quartz enhanced photoacoustic gas sensing, Freiburg Infrared Colloquium, 2017
4) Spagnolo, V., Sampaolo, A., Patimisco, H., Giglio, M., Tittel, F.K., Quartz-enhanced photo-acoustic spectroscopy with QCLs, International Training School - Beyond Conventional Tissue Imaging, COST 2017